

Spin-orbit Splitting in the Conduction Subband of Semiconductor Asymmetric Heterostructures

Erasmio A. de Andrada e Silva

Instituto Nacional de Pesquisas Espaciais - INPE

C.P. 515, 12201 São José dos Campos, S.P., Brazil

Received July 21, 1995

It is presented here a study of the spin-orbit splitting in the electronic subbands of asymmetric semiconductor heterostructures, due to the lack of mirror symmetry along the growth direction. From the multi-band Kane model, the limits of validity of the popular one-band effective mass Rashba model Hamiltonian are discussed and the breakdown of the so called Ando's argument against the splitting is explained. It is shown in particular that the spin-orbit parameter α_{so} is not proportional to the average electric field. The splitting anisotropy in k -space and the spin relaxation are also considered in connection with recent experiments.

I. Introduction

Contrary to the case of holes, the spin-orbit splitting in the conduction subband of narrow gap semiconductor heterostructures has been a controversial issue for more than twenty years now. New and more precise experiments probing the spin dependent static and dynamic properties of heterostructures have recently renewed the interest in the electron zero-field spin splitting problem^[1-4], which is not fully understood yet.

Such spin-orbit splitting in the conduction subband originates from the structure's lack of mirror symmetry along the growth direction as well as from the lack of inversion symmetry in the microscopic bulk potential of the III-V host semiconductor^[2-5]. The spin-orbit splitting due to mirror asymmetry in the confining potential was first described by Rashba^[6]. He introduced a simple one band effective mass model, which has since then been widely used to interpret the results of different experiments^[6-8]. Many are the evidences to believe that the Rashba term gives the bigger contribution to the splitting in the case of narrow-gap heterostructures^[2,5,8-10]. This term is however also the one at the center of the discussion.

The first experimental attempts to estimate the splitting obtained values that were much smaller than those calculated theoretically^[7,11-13]. A simple qualitative argument by Ando put in check the first calcu-

lations and seemed to support the experimentalists^[14]. Ando's reasoning follows roughly as: as the spin-orbit splitting results from the relativistic effect in which a moving electron with nonzero k sees in its reference frame the interface electric field transformed into a magnetic field, it should be very small for the confined states, since they see an average electric field equal to zero.

Such argument was shown later to be oversimplified, in part in view of the later more accurate measurements in which large splittings were observed with different techniques and in different structures^[3,7,10]. The only existing formal comment on the so called Ando's argument consists in the observation that, in the case of a position dependent effective mass, because of the special boundary conditions, the effective mass equation for the confined states, contrary to a true Schrödinger equation, does not lead to the zero average electric field condition^[15,16]. Without entering into the problem of boundary conditions we show why such argument breaks down.

We use the eight-band Kane model to derive and discuss the limits of validity of the popular one band effective mass Rashba model Hamiltonian. In the next section we present the model and the splitting calculation. The solution with a hypothetical mirror asymmetric quantum well (QW) exemplifies the breakdown

of the Ando's argument. Before the conclusion, we briefly consider the magneto-oscillations, the splitting anisotropy and the spin relaxation, all in connection with recent experiments.

II. Conduction subband spin-orbit splitting

Two-dimensional electrons are usually described with spin degenerate quantized sub-bands. The first relativistic correction, represented by the spin-orbit coupling term in the Schrödinger equation, lifts the degeneracy of the non-zero wave vector states whenever the structure is asymmetric or based on inversion asymmetric bulk semiconductors. Here we are concerned with the theory of this effect.

In the case of symmetric quantum wells, the spin-orbit splitting is only due to the bulk asymmetry, and can be taken into account within first-order perturbation theory by simply computing the expectation value of the so called k^3 bulk term^[17] with the unperturbed subbands^[18,19].

A. Rashba model Hamiltonian

The problem of the splitting in the case of asymmetric semiconductor heterostructures is a more difficult one. As mentioned above, there is a popular model Hamiltonian to describe the experiments which reads:

$$H = \frac{\hbar^2 k^2}{2m^*} + \alpha_{so}(\mathbf{k} \times \hat{\mathbf{z}}) \cdot \boldsymbol{\sigma}, \quad (1)$$

where $\boldsymbol{\sigma} = \sigma_x \hat{\mathbf{x}} + \sigma_y \hat{\mathbf{y}} + \sigma_z \hat{\mathbf{z}}$ is the Pauli matrices vector, $\hat{\mathbf{k}}$ is the unit vector along the growth direction and α_{so}

is a structure parameter, sometimes called spin-orbit coupling parameter.

This Hamiltonian for the parallel motion with spin-orbit interaction was proposed by Rashba for the 2D case using general symmetry arguments^[6]. The problem of the motion along the growth direction is assumed to be separated. The parameter α_{so} has been determined experimentally, but comparison with theory has not been easy^[3,20]. We obtain α_{so} from the eight-band Kane model.

B. $k \cdot p$ model

Working within the effective mass approximation we start from the analytic $k \cdot p$ model for the bulk dispersion relations. We consider III-V semiconductor compounds described by the eight-band Kane model. Making use of its spherical symmetry, we choose the parallel wave vector \vec{k} along the x axis, so that the electron wave function will be given by:

$$\psi(\vec{r}) = e^{ikx} \sum_{j=1}^8 f_j(z) u_j(\vec{r}), \quad (2)$$

where the f_j are the envelope functions and the u_j are the bulk Bloch functions at the zone center as in Ref. [2]. They diagonalize the bigger, and the only one considered here, term in the spin-orbit coupling. The effective-mass Hamiltonian is block-diagonalized with the following two 4×4 blocks corresponding to the two electron or conduction subband spin state

$$H_{\pm} = \begin{pmatrix} E_c[z] + V(z) & P \left(\frac{d}{dz} \mp \frac{k}{2} \right) & \mp \frac{\sqrt{3}}{2} P k & \frac{P}{\sqrt{2}} \left(\frac{d}{dz} \pm k \right) \\ P \left(-\frac{d}{dz} \mp \frac{k}{2} \right) & E_v[z] + V(z) & 0 & 0 \\ \mp \frac{\sqrt{3}}{2} P k & 0 & E_v[z] + V(z) & 0 \\ \frac{P}{\sqrt{2}} \left(-\frac{d}{dz} \pm k \right) & 0 & 0 & E_v[z] - \Delta[z] + V(z) \end{pmatrix}, \quad (3)$$

where $V(z)$ is the electrostatic space-charge or applied external potential, the momentum matrix element $P = \sqrt{\frac{2}{3}} \frac{\hbar}{m_e} \langle iS | p_x | X \rangle$ (m_e being the bare electron mass) and $E_c[z]$, $E_v[z]$ and $\Delta[z]$ represent the energy position of the band edges and the value of the spin-orbit valence band energy splitting in the differ-

ent semiconductor layers along the z direction. The k^2 free particle term in the diagonal matrix elements is neglected.

As in Ref. [2] we can eliminate the valence band envelope functions from the multi-band effective-mass equation and obtain the following Schrödinger like

equation for the conduction band components:

$$\left[-\frac{\hbar^2}{2} \frac{d}{dz} \frac{1}{m(z, \epsilon_{\pm})} \frac{d}{dz} + \frac{\hbar^2 k^2}{2m(z, \epsilon_{\pm})} + E_c[z] + V(z) \mp \alpha(z, \epsilon_{\pm})k - \epsilon_{\pm} \right] f_{\pm} = 0, \quad (4)$$

with

$$\frac{1}{m(z, \epsilon_{\pm})} = \frac{P^2}{\hbar^2} \left(\frac{2}{\epsilon_{\pm} - V(z) - E_v[z]} + \frac{1}{\epsilon_{\pm} - V(z) - E_v[z] + \Delta[z]} \right) \quad (5)$$

and

$$\alpha(z, \epsilon_{\pm}) = \frac{P^2}{2} \frac{d}{dz} \left(\frac{1}{\epsilon_{\pm} - V(z) - E_v[z]} - \frac{1}{\epsilon_{\pm} - V(z) - E_v[z] + \Delta[z]} \right), \quad (6)$$

where ϵ_{\pm} are the spin dependent eigen energies, $|\epsilon_+ - \epsilon_-|$ being the spin splitting; they all of course depend on the parallel wave vector k .

Note that the Kane model gives no bulk spin splitting. The bulk k^3 term comes from the interaction with remote bands. Note also that the Rashba splitting proportional to α and to k is zero in the bulk ($V(z) = const.$) and when $\Delta = 0$. The spin-coupling parameter in the Rashba model is then seen to be given by $\alpha_{so} = \langle \alpha(z, \epsilon_0) \rangle$, where $\langle \rangle$ means expectation value in the unperturbed subband with energy ϵ_0 .

C. Results

Fig. 1 shows the splittings obtained for both InAs and GaSb heterojunctions with other large gap materials. Equation (4) is solved variationally in the infinite barrier approximation^[2]. The spin-orbit splitting at the Fermi "surface" is plotted as a function of the surface carrier density n_s . The splitting is shown for k_f along three different directions. The anisotropy we see is due to the presence of the bulk k^3 term included within first order perturbation theory as mentioned above, and will be further discussed below.

Following Ando's reasoning however one could think that without wave function barrier penetration, as in the infinite barrier approximation, the splitting would be overestimated. Avoiding the problem of boundary conditions, we address this question by considering

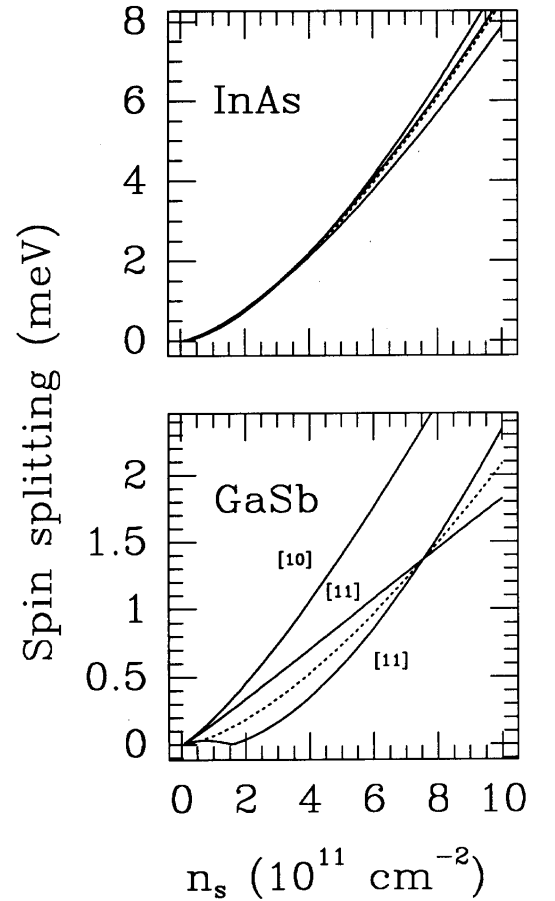


Figure 1. Spin-orbit splitting at three points of the Fermi "surface" along different directions in k -space (indicated in the case of GaSb), as a function of the carrier density n_s . The dashed line gives the isotropic contribution of the Rashba term alone. Only the first subband is occupied.

an infinite semiconductor under the following applied hypothetical external QW^[21]

$$V(z) = V_0(1 - e^{(z/c(z))^2}), \quad (7)$$

where $c(z) = a\Theta(-z) + b\Theta(z)$; $\Theta(z)$ is the Heaviside function. This is a simple continuous potential well with continuous derivative, where the difference between parameters a and b gives the degree of its mirror asymmetry at $z = 0$. With such a potential we solved Eq. (4) and in Fig. 2 we show the obtained splittings for the cases of fixed $b = 100\text{\AA}$ and $a = 90, 10$ and 5\AA .

We first note that the $a = 90\text{\AA}$ quasi-symmetric case leads in fact to very small splittings and that the splitting grows with decreasing a as a result of the increasing mirror asymmetry (and confinement). The small a case resembles an abrupt interface. We also note that, in agreement with other multiband calculations^[13,20,22,23], the spin splitting grows initially linearly with k and then tends to saturate. The most interesting conclusion one can draw from these results comes however from the comparison with the infinite barrier case, also plotted in Fig. 2. Contrary to the common expectation one sees only a small difference between the small a case and the no penetration infinite barrier case.

One can understand the above numerical results by having a closer look at the analytic expression for the z and energy dependent Rashba spin-orbit parameter α . To simplify we set $\Delta = \infty$ and work within the 6×6 model. The reasoning and conclusions for the more ac-

curate 8×8 model are exactly the same. By noting that for the confined electrons in Type I structures, as considered here, $\epsilon_{\pm} - V(z)/E_g$ is always less than one, we can write (6) as

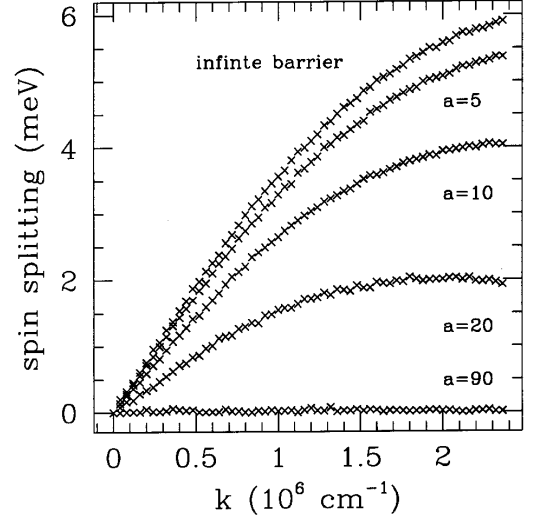


Figure 2. Splittings obtained with the asymmetric potential well in equation (7). The bulk parameters are those of InAs and $V_0 = 400$ meV. We have set $b = 100\text{\AA}$ and plotted the results for different values of a in \AA . The solution with an infinite barrier at $z = 0$ is also shown.

$$\alpha(z, \epsilon_{\pm}) = \frac{P^2}{2E_g^2} \left[1 - 2 \left(\frac{\epsilon_{\pm} - V(z)}{E_g} \right) + 3 \left(\frac{\epsilon_{\pm} - V(z)}{E_g} \right)^2 - \dots \right] eE, \quad (8)$$

where $eE = \frac{d}{dz}V(z)$ and we have set $E_c = 0$ and $E_v = -E_g$ for small values of k , in the well region we have for the localized states in general $\epsilon_{\pm} - V(z)/E_g$ much smaller than one and, in this case, the first term above gives a good approximation to the infinite series. The coupling parameter in the Rashba Hamiltonian only in this case can be approximated by

$$\alpha_{so} = \alpha_0 \langle E(z) \rangle, \quad (9)$$

where $\langle E(z) \rangle$ is the average electric field. This approximation will work well whenever the electron is mainly localized in the well and the penetration of the wave function in the barrier can be neglected. The parameter α_0 in the eight-band model is given by^[2]

$$\alpha_0 = \frac{\hbar^2}{2m^*} \frac{\Delta}{E_g} \frac{2E_g + \Delta}{(E_g + \Delta)(3E_g + 2\Delta)} e. \quad (10)$$

In table I we list the values of α_0 for different III-V compounds.

TABLE 1. Spin-orbit coupling parameter α_0 , as given by Eq. (10), for different III-V semiconductor compounds. The bulk parameters used are those from the Numerical Data and Functional Relationships in Science and Technology, eds O. Madelung, M. Schultz and M. Weiss. Landolt-Bornstein (Spring-Verlag, Berlin 1982).

	GaAs	InSb	InAs	GaSb
$\alpha_0 (e\text{\AA}^2)$	6.0	498	114	33.1

III. Experiments

The experimental evidences and studies of the conduction subband spin-orbit splitting have been of mainly three types:

A. Magneto-oscillations

As in the bulk, the observed beating pattern in the magneto oscillations (Shubnikov-de Haas, de Haas-van Alphen, etc.) was the first clear manifestation of the spin splitting in the conduction subband of asymmetric semiconductor heterostructures. It was observed by different groups in different structures^[8,9,24].

The theory was given in Ref. 2. We give here just a brief outline. It starts with the determination of the eigenstates in the presence of an external magnetic field applied perpendicularly to the interface. The Hamiltonian projected into the 2×2 conduction band space reads^[2]

$$H = \begin{pmatrix} \epsilon(k) + \frac{1}{2}\mu g^*(k)B & \gamma\Omega(\vec{k}) + i\alpha_{so}k_- \\ \gamma\Omega^\dagger(\vec{k}) - i\alpha_{so}k_+ & \epsilon(k) - \frac{1}{2}\mu g^*(k)B \end{pmatrix}, \quad (11)$$

where $\vec{k} = i\nabla + \frac{e}{\hbar}\vec{A}$, \vec{A} being the vector potential of the applied field; $\epsilon(k)$ is the single particle spin independent nonparabolic energy dispersion relation; μ is the Bohr magneton; $g^*(k)$ is the k -dependent effective g -factor; $k_\pm = k_x \pm ik_y$; γ is the bulk k^3 material parameter and

$$\Omega(\vec{k}) = \frac{1}{4}(k_+k_-k_+ - k_-^3) - k_+q, \quad (12)$$

with $q = \langle -\frac{d^2}{dz^2} \rangle$. The two terms in the off-diagonal matrix elements represent the two mentioned contributions to the splitting.

With the numerical diagonalization of the above Hamiltonian the magneto-oscillations can be more easily obtained by calculating the magnetization of the two-dimensional electron gas (2DEG). The magnetization as a function $1/B$ presents periodic modulated oscillations. In Fig. 3 we show, together with their power spectrum, the oscillations obtained for InAs heterojunctions with different carrier densities. The power spectrum is the absolute value squared of the Fourier transform of the magnetization and is shown in units of surface densities. As given from the semiclassical expression $\nu = n_s \hbar \pi / e$, the frequency in Tesla is

$\nu[T] = 4.13n_s[10^{11}\text{cm}^{-2}]$. One should first note that the oscillations in $1/B$, within this range of carrier concentration, present a quite regular beating pattern. The power spectrum shows two near frequencies corresponding to the total number of carriers which occupy the two spin-split subbands. Such frequencies occur at

$$n_\pm = \frac{1}{(2\pi)^2} \int d\vec{k} \Theta(\epsilon_F - \epsilon_\pm(\vec{k})); \quad (13)$$

which are the densities in the split bands. Their separation produces the beatings, which increase with total carrier density as a result of the increasing spin-splitting at the Fermi energy shown in Fig. 1.

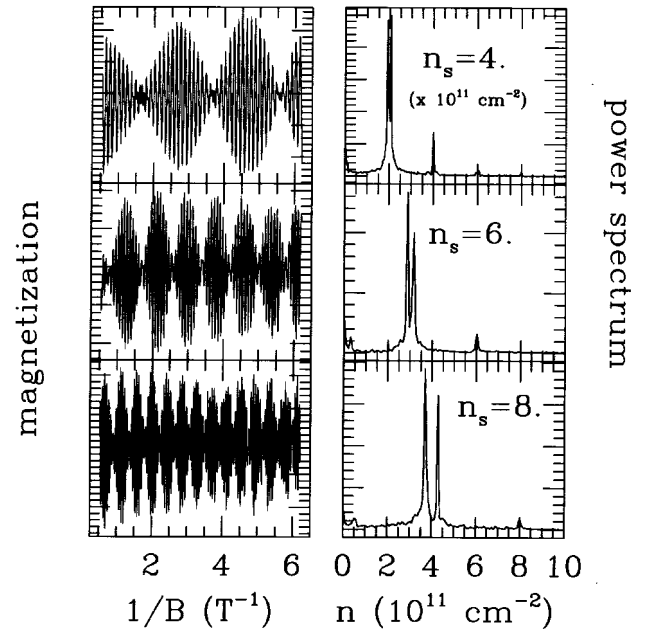


Figure 3. Obtained oscillating magnetization of the 2DEG at the interface of an InAs based heterojunction with varying carrier concentration n_s . On the left panel the beating pattern is clearly evident. On the right panel we plot the respective power spectrum in terms of surface density n . The oscillation frequencies are shown as strong peaks.

The regular beating pattern in Fig.3 is a result of the dominant Rashba contribution. The same regular beating was observed experimentally with different asymmetric structures where the Rashba term dominates^[8,9]. It was shown in Ref. [2] that a strong anisotropy in the splitting will lead to anomalous beating pattern in the magneto oscillations, but it has not been observed yet.

B. Raman scattering

The most direct observation of the spin-orbit splitting has been with Raman scattering experiments^[3,25].

With this technique the k -space anisotropy, as predicted in Ref. [19], was first observed. The total spin splitting is given by

$$\Delta_s(k, \theta) = 2 \left[(\gamma^2 q^2 + \alpha^2) k^2 + \gamma \alpha (k^2 - 2q) k^2 \sin 2\theta + \gamma^2 (k^2 - 4q) \frac{k^4}{4} \sin^2 2\theta \right]^{1/2}, \quad (14)$$

where θ is the angle between the parallel wave vector \vec{k} and the x axis of the cubic crystal. This expression has been confirmed by first principle tight-binding calculations and agrees with the observed splittings for electrons moving along different directions in a GaAs asymmetric QW^[3].

In Ref. [3] a spin-orbit coupling parameter $\alpha_{so} = -6.9 \pm 0.4$ meV \AA was determined. The sample used was an asymmetrically doped thick GaAs quantum well (negligible barrier penetration). The self consistent average space-charge electric field was calculated to be $\langle E(z) \rangle = -1.06$ mV/ \AA , what leads to $\alpha_0 = 6.5 \pm 0.4$ e \AA^2 . Eq. (10) gives a theoretical value of 6.0 e \AA^2 . Considering more conservative uncertainties in the experiment and uncertainties in the material parameters entering the theoretical value, we have here a very good agreement between experiment and theory.

C. Anti-localization

Another set of experiments that probe the spin-orbit splitting makes use of the quantum transport effect known as anti-localization. The spin dephasing responsible for the observed negative magnetoresistance (due to antilocalization) has been shown to be due to the precession of the electron spin around the spin splitting effective magnetic field^[10,26]. The spin dephasing rate in this case follows the following motional narrowing law^[27]

$$t_s^{-1} = a \frac{\langle \Delta_s^2 \rangle}{4\hbar^2} t^*, \quad (15)$$

where $\langle \rangle$ means now average over the Fermi “surface”, t^* is the transport (or elastic) scattering time and a is a parameter of the order of unit that depends on the scattering mechanism.

In Fig. 4 we plot the average Dyakovov-Perel spin relaxation time t_s for the electrons at the Fermi “surface” of an AlGaAs/GaAs heterojunction, as a function of the carrier density. Both contributions to

the spin-orbit splitting are important and have been included^[2,4]. We can see that t_s is strongly dependent on the energy of the electron. One goes from almost no relaxation in the empty band limit to very high relaxation rates as the energy (and the splitting) increases. The interpretation of the experimental data is however not simple and is still under discussion^[4].

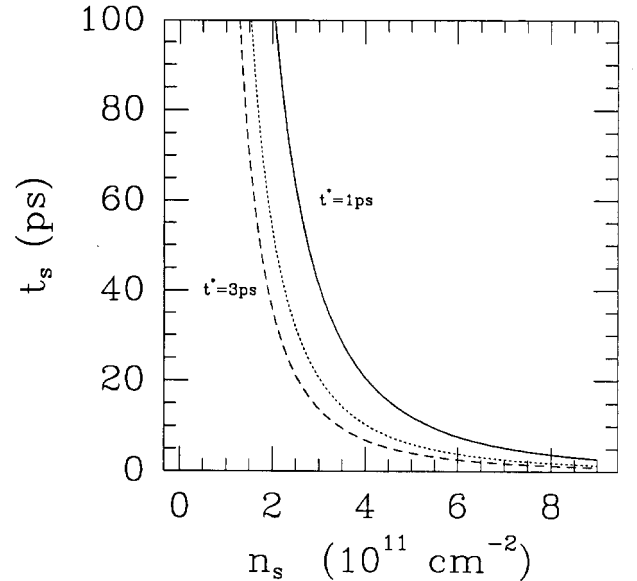


Figure 4. Average D'yakonov-Perel electron spin relaxation time t_s at the Fermi “surface” of an AlGaAs/GaAs heterojunction with varying carrier concentration n_s . We used $a = 0.5 = 17$ eV \AA^3 and varied t^* between 1 and 3 ps.

IV. Conclusions

We can briefly summarize our results as follows. We have obtained from an eight-band Kane model the spin-orbit splitting in the electronic subbands of asymmetric QWs. We have made the connection with the Rashba model and shown that the spin-orbit coupling parameter is approximately proportional to the average electric field only when wave function barrier penetration can be neglected. The values of the parameter for different III-V semiconductors have been given. One should also keep in mind that the Rashba spin-orbit coupling and the nonparabolicity corrections in the conduction subband are of the same order of magnitude^[28]. Therefore a consistent and more precise Rashba model should have a nonparabolic kinetic term replacing the parabolic one in Eq. (1). The D'yakonov-Perel electron spin relaxation time was shown to be highly dependent

on the electron's energy. Finally we have also reviewed the main experiments, which show a fairly good agreement with the theory presented.

Acknowledgments

The author wishes to acknowledge Profs. F. Bassani and G. La Rocca for the collaboration and guidance in the spin splitting problem and for the kind hospitality in Pisa where most of this work was done.

References

1. A. Vinattieri et al. Phys. Rev. **B50**, 10868 (1994), and references there in.
2. E. A. de Andrada e Silva, G. C. La Rocca and F. Bassani, Phys. Rev. **B50**, 8523 (1994).
3. B. Jusserand, D. Richards, G. Allan, C. Priester and B. Etienne. Phys. Rev. B **51**, 7107 (1995).
4. F.G. Pikus and G.E. Pikus, Phys. Rev. **B51**, 16928 (1995).
5. G. Lommer, F. Malcher, and U. Rossler, Phys. Rev. Lett. **60**, 728 (1988).
6. Yu. A. Bychkov and E. I. Rashba, Pis'ma Zh. Eksp. Teor. Fiz. **39**, 66 (1984) [JETP Lett. **39**, 78 (1984)]; J. Phys. C **17**, 6039 (1984).
7. R. Wollrab, R. Sizmann, F. Koch, J. Ziegler, and H. Maier, Semicond. Sci. Technol. **4**, 491 (1989).
8. J. Luo, H. Munekata, F. F. Fang and P.J. Stiles, Phys. Rev. B **41**, 7685 (1990).
9. B. Das, D. C. Miller, S. Datta, R. Reifenberger, W. P. Hong, P. K. Bhattacharya, J. Singh and M. Jaffe, Phys. Rev. **B39**, 1411 (1989).
10. S. K. Greene, J. Singleton, P. Sobkowicz, T.D. Golding, M. Pepper, J.A. Perenboom and J. Dinan, Semicond. Sci. Technol. **7**, 1377 (1992).
11. D. Stein, K. von Klitzing and G. Weimann. Phys. Rev. Letters **51**, 130 (1983).
12. F.J. Ohkawa and Y. Uemura, J. Phys. Soc. Jpn. **37**, 1325 (1974); Y. Takada, K. Arai, N. Uchimura and Y. Uemura, J. Phys. Soc. Jpn. **49**, 1851 (1980).
13. G. E. Marques and L.J. Sham, Surf. Sci. **113**, 131 (1982).
14. A. Därr, J.P. Kotthaus and T. Ando, Proc. of the 13th International Conference on the Physics of Semiconductors, Rome, Italy, 1976, Ed. F.G. Fumi (North Holland, Amsterdam, 1977), p. 774.
15. F. Malcher, G. Lomer and U. Rössler, Superlatt. Microstructures **2**, 267 (1986).
16. G.L. Chen, J. Han, T.T. Huang, S. Datta and D.B. Janes, Phys. Rev. **B47**, 4084 (1993).
17. G. Dresselhaus, Phys. Rev. **100**, 580 (1955).
18. R. Eppenga and M.F.H. Schuurmans, Phys. Rev. B **37**, 10923 (1988).
19. E.A. de Andrada e Silva, Phys. Rev. B **46**, 1921 (1992).
20. R. Winkler and U. Rossler, Phys. Rev. **B48**, 8918 (1993).
21. E. A. de Andrada e Silva and G. C. La Rocca, unpublished.
22. I. Nachev, Semicond. Sci. Technol. **3**, 29 (1988).
23. P. Sobkowicz, Semicond. Sci. Technol. **5**, 183 (1990).
24. Yu. L. Ivanov, P. Kop'ev, S. Suchalkin and V. Ustinov, JETP Lett. **53**, 493 (1991).
25. D. Richards, B. Jusserand, H. Peric, and B. Etienne, Phys. Rev. B **47**, 16028 (1993).
26. P. D. Dresselhaus, C.M. Papavassiliou, R.G. Wheeler and R.N. Sacks, Phys. Rev. Lett. **68**, 106 (1992).
27. M. I. D'yakonov and V. I. Perel, Sov. Phys. JETP **33**, 1053 (1971).
28. This can be seen by comparing the expansion (8) with the similar one for the energy dependent effective mass, as first pointed out in reference 2.